



Research article

Occurrence, transformation, and transport of PFAS entering, leaving, and flowing past wastewater treatment plants with diverse land uses



Kyra Sigler, Tiffany L. Messer ^{*}, William Ford, Wayne Sanderson

Biosystems and Agricultural Engineering, University of Kentucky, Lexington, KY, USA

ARTICLE INFO

Handling editor: Prof Raf Dewil

Keywords:

Transformation and transport
PFAS
Wastewater treatment
Biosolids

ABSTRACT

Per- and polyfluoroalkyl substances (PFAS) have been detected ubiquitously throughout the environment. Wastewater treatment plants (WWTPs) have been identified as potential hotspots for the introduction of PFAS into the environment. Therefore, the occurrence, transformation, and transport of 18 PFAS in two WWTPs with varying treatment processes, prevailing land uses, and during two distinct time periods were investigated. Polar Organic Chemical Integrative Samplers (POCIS) were installed at two WWTPs in Central Kentucky during April and July of 2022. PFAS concentrations typically increased from influent to effluent at both WWTPs, regardless of wastewater treatment processes, but changes in surface water concentrations from upstream to downstream of the effluent mixing zones varied. Both WWTPs discharged the 18 PFAS at higher loads than received, indicating prevalent transformation of PFAS precursors and non-measured PFAS analytes into measurable PFAS. Nearly all measured PFAS persisted in aqueous (86–98%) compartments rather than sediment or biosolids (2–14%). All biosolids had low content of PFAS with the dominant compound being PFOS (1.59–2.60 ng/g). Based on recent US EPA proposed maximum contaminant levels, hazard indexes for drinking water were exceeded in effluent and downstream surface waters at both WWTPs. The WWTP located in a heavily developed area and downstream from a firefighting training facility, had significantly higher concentrations of most PFAS species at most monitoring sites and was less impacted by sampling period compared to the WWTP located in a moderately developed, pastured area. Findings support the importance of WWTPs and land use practices as contributing to PFAS impact to downstream ecosystems along with potentially increasing strains on downstream drinking water source waters in regions that are surface water dependent.

1. Introduction

Per- and polyfluoroalkyl substances (PFAS) are a class of man-made chemicals developed in the 1940s and 1950s (Buck et al., 2011). They provide water, dirt, oil, and grease repellent properties; thus, they are found in many products including textiles, papers, metals, wires, firefighting foams, and nonstick cookware (Kirk et al., 2018; Kwiatkowski et al., 2020). Their high chemical, thermal, and biological stability result in extreme persistence once released into the environment (Buck et al., 2011; Kwiatkowski et al., 2020). Further, the wide application of PFAS in consumer products has led to background concentration exposure to the public (Kirk et al., 2018). PFAS are ubiquitous in human blood serum and have been linked to health effects, including high cholesterol, kidney and testicular cancer, decreased vaccination response in children, developmental delays, and thyroid disease (Brase et al., 2021; Kirk et al., 2018; Kwiatkowski et al., 2020; Steenland and Winquist, 2021).

PFAS have been detected around the world in many environmental compartments including soil, surface water, sediment, groundwater, and finished drinking water (Bai and Son, 2021; Bao et al., 2019; Brase et al., 2021; Department for Environmental Protection, 2019; Goodrow et al., 2020; Kwiatkowski et al., 2020; Sardina et al., 2019; Sim et al., 2021). They appear to be more frequent in residential and industrial areas, indicating urban areas as hotspots for the introduction of PFAS into the environment (Sardina et al., 2019; Sim et al., 2021). Other trends in PFAS contamination depend on their carbon chain length and PFAS group (i.e. PFCAs, PFSAs, PFESAs). Long chain PFAS have a higher affinity for adsorption to particulate matter, thus they are observed more in soil, sediment, and plant roots while short chain PFAS are highly soluble in water and are observed more in aqueous compartments and plant shoots (Bai and Son, 2021; Dahleh et al., 2018; Goodrow et al., 2020; Sardina et al., 2019). The PFAS group perfluorinated alkyl acids (PFAAs), which include perfluorinated carboxylic acids (PFCAs) and

* Corresponding author.

E-mail address: Tiffany.Messer@uky.edu (T.L. Messer).

perfluorinated sulfonic acids (PFSAs), are observed at higher concentrations compared to other PFAS groups, including perfluoroalkyl ether acids and PFAS precursors, as these other groups often degrade into PFAAs (Y. Wang et al., 2022).

PFAS have the potential to be directly ingested into the human body through contaminated water, crops, and animals. A 2019 evaluation of Kentucky's drinking water found PFAS in 15% of finished drinking water samples, with the most common PFAS compounds detected being the legacy compounds PFOS and PFOA (Department for Environmental Protection, 2019). Further, PFAS undergo biomagnification in the aquatic food chain, leading to increasing concentrations as the trophic levels progress and have been observed to accumulate in plants, macroinvertebrates, fish, amphibians, and higher order predators including whales, birds, and humans (Brase et al., 2021; Flynn et al., 2021; Goodrow et al., 2020; Koch et al., 2020; Kwiatkowski et al., 2020; D. Q. Zhang et al., 2020). One of the most common exposure pathways to the public is through specific community exposure (i.e., through industrial emissions, landfill leachate, or PFAS contaminated run-off into surface waters) (Olsen, 2015). A potential transport route for these contaminants to surface water includes effluent leaving wastewater treatment plants and land applied biosolids (Cui et al., 2020; Masoner et al., 2020; Podder et al., 2021).

Because of the novelty of PFAS as a contaminant of concern, wastewater treatment plants (WWTPs) are not designed to remove PFAS from influent, often resulting in measured effluent concentrations exceeding influent concentrations (Coggan et al., 2019; Dalahmeh et al., 2018; Hamid and Li, 2016; Lenka et al., 2021). This is attributed to transformation of PFAS precursors and polyfluorinated alkyl substances into terminal, perfluorinated alkyl substances during the WWTP process (Y. Wang et al., 2022; Xiao et al., 2018). While this increase in PFAS concentration has been repeatedly observed around the world, there has been limited investigations explicitly comparing distinct treatment processes, such as disinfection method, on PFAS transformations in WWTPs. One example is Pan et al. (2016), who observed percent decreases of 3.6% and 11% during UV disinfection and a percent increase of 29% during Cl₂ disinfection for the sum of 18 PFAS at three different WWTPs in south China; however, only a single 24-h composite sample was collected at each site, thus temporal variability that may have occurred throughout the year was not considered.

Further, the ineffectiveness of PFAS treatment in WWTPs allows PFAS to leave the plant in either effluent or municipal biosolids; the former of which can reintroduce PFAS into urban water systems and downstream drinking water sources and the latter introduces PFAS into agricultural landscapes (Cui et al., 2020). Despite the overwhelming evidence of PFAS in WWTP effluent, few studies have simultaneously investigated PFAS presence in WWTPs and in immediate surface water and sediment downstream of the effluent mixing zone. Therefore, a better understanding of the presence and transformation of PFAS once discharged from WWTPs is still needed.

Ultimately, the presence of these contaminants in WWTP effluent may propagate unintended environmental consequences and human exposure, leading to severe ecological and human health impacts. Therefore, the goal of this study was to investigate the occurrence and temporal variability of PFAS in two WWTPs of varying land use, treatment capacity, and treatment processes in order to identify trends that will guide future PFAS management. The overall objectives were to quantify the impact of WWTP effluent on downstream surface waters and sediment concentrations of PFAS and to gain a better understanding of PFAS transformation and presence in WWTP influent, effluent, and biosolids.

2. Materials and methods

2.1. Analytes

In this study, 18 unique PFAS analytes were investigated, whose

groups, subgroups, and chemical characteristics can be found in Table S1. A Polar Organic Chemical Integrative Sampler (POCIS) is a passive sampler capable of measuring time-weighted average (TWA) concentrations for a suite of emerging contaminants like pharmaceuticals, pesticides, hormones, and PFAS at concentrations as low as parts per trillion. The 18 analytes in this study were chosen based on the analytical capabilities for POCIS extracts in surface and wastewater matrices at the time of the study and were analyzed using methods developed by the Nebraska Water Sciences Laboratory specifically for POCIS extracts (Caniglia et al., 2022) and included analytes recently proposed by the US EPA to have reduced maximum contaminant levels (MCLs) and hazard indexes (HIs) for drinking water (U.S. Environmental Protection Agency Office of Water (4304T) & Office of Science and Technology Health and Ecological Criteria Division, 2023). The region of the study uses surface water as the primary drinking water source, putting unique challenges on downstream users.

Analytical grade standards were purchased from Wellington Laboratories, USA for the 18 PFAS that have previously been investigated using POCIS: perfluoroalkyl ether carboxylic acids (PFECA), polyfluoroalkyl ether sulfonates (PFES), perfluorinated sulfonic acids (PFSA), perfluorinated carboxylic acids (PFCA), and PFAS precursors. Three isotope-labeled internal standards (IS) were obtained from Wellington Laboratories, USA, d3-NMeFOSAA, 13C4-PFOS, and 13C2-PFOA, as well as four isotope-labeled surrogates, 13C2-PFHXA, 13C3-HFPO-DA, 13C2-PFDA, and d5-NEtFOSAA. Standards and surrogates were mixed into a concentrated high purity methanol solution ($\geq 99.99\%$, Honeywell CHROMASolv LC-MS) purchased from Midland Scientific Corporation, USA. Tetra-butylammonium hydrogen sulfate (TBAS), sodium carbonate (Na₂CO₃), and sodium hydroxide (NaOH) were all purchased from Aldrich Chemical (Milwaukee, WI, USA), while methyl tert-butyl ether (MTBE), formic acid, and acetonitrile (ACN) were purchased from Fisher Scientific (Pittsburg, Pennsylvania, USA). Highest purity nitrogen and argon gas ($>99.99\%$) were used. Details for quality assurance and control can be found in Supplemental Material.

2.2. Site descriptions

2.2.1. Wastewater treatment plants (WWTPs)

WWTP1 was located in an urban area of Central Kentucky and served an estimated $\sim 130,000$ people. It was designed to treat 30 million gallons of wastewater per day (MGD) with a maximum capacity of 60 MGD and average flow of 22 MGD (Kentucky Infrastructure Authority Office of the Governor, 2021). WWTP2 was located in a rural area of Central Kentucky and served approximately 26,000 residents. The plant had a design capacity of 7.2 MGD, a maximum capacity of 24 MGD, and an average flow of 4 MGD (Kentucky Infrastructure Authority Office of the Governor, 2022). Several differences existed between the WWTPs including WWTP1 having an additional clarifier, aeration biological treatment basin, and chlorine disinfection compared to the WWTP2 having an anaerobic biological selector and UV disinfection (Fig. 1). Ideally, both treatment plants would have had the same construct with exception to one treatment process; however, that was not possible in the region of this study. Both WWTPs received industrial, residential/domestic, and commercial wastewater and required industrial pre-treatment of wastewater.

2.2.2. Stream sites

Receiving surface waterways at each WWTP had an upstream and downstream site where surface water and sediment samples were collected. Watershed sizes were determined using ArcGIS Pro 3.1.0 (2023) and were 19.6 km² and 29.2 km² at the downstream sites for WWTP1 and WWTP2, respectively. At WWTP1, the approximate distance between the upstream site and effluent mixing zone (EMZ) was 0.56 km and the approximate distance between the EMZ and the downstream site was 0.26 km (Fig. S1A). At WWTP2, the distances were 0.22 km from the upstream site to the EMZ and 0.23 km from the EMZ to

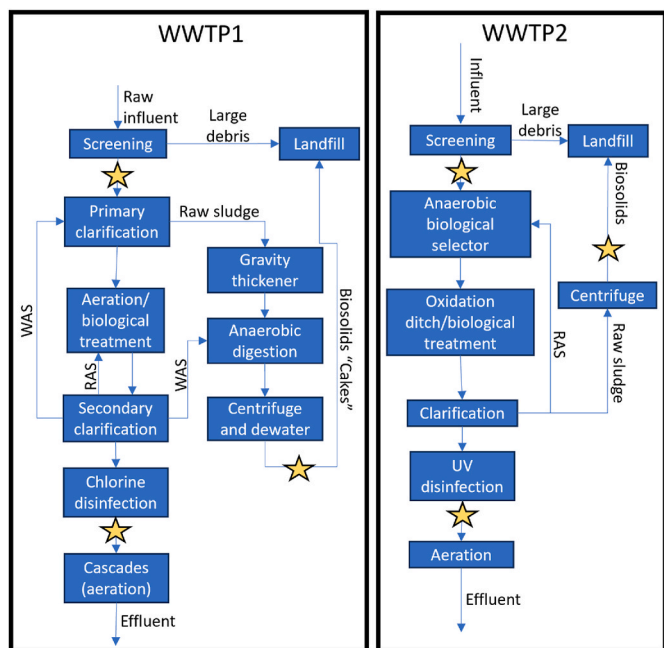


Fig. 1. General treatment processes at WWTP1 and WWTP2. WAS = waste activated sludge. RAS = return activated sludge. Unlabeled arrows represent the flow of water. Stars indicate sampling locations. *Note following aeration in WWTP2 effluent was discharged to a storage pond, which only released to the downstream location in high flow events or when the pond reached its maximum storage volume.

the downstream site (Fig. S1B). Water depth and temperature were monitored at 10-min intervals using a HOBO U20L-04 (Onset, Bourne, MA). Data loggers were attached to cinderblock secured in place using steel rebar rods midstream. Stream cross sections and longitudinal slopes (S) at stream locations were obtained using a SAL Series 24X Automatic Level (Robert Bosch Tool Corporation, Michigan, USA). The depth recordings were used in conjunction with the surveyed cross sections to calculate cross sectional area (CSA), wetted perimeter, and hydraulic radius (R) for 10-min intervals for each deployment period. WWTP2 site had a water control structure directly downstream of the downstream monitoring location, which slowed water movement resulting in more flow upstream compared to downstream flow.

2.2.3. Land cover

Land cover data was obtained from the National Land Cover Dataset (NLCD) (USDA, 2022) and was analyzed in ArcGIS Pro 3.1.0 (2023). WWTP1's watershed was 97% developed. The remaining 3% was pasture/hay and forest. WWTP1's sewershed, the pipe network connected to the WWTP, was also primarily developed land (79%), but had 16% pasture/hay and 3% forest. WWTP2's watershed included 53% developed and 41% pasture/hay, while its sewershed included 59% developed and 35% pasture/hay.

2.3. Sample collection and analysis

2.3.1. Pre-deployment cleaning

Due to the high potential of PFAS contamination, all materials were meticulously cleaned prior to deployment. Any materials that would encounter water, sediment, or solids that would be tested for PFAS were cleaned with Liquinox according to the manufacturer's instructions then triple rinsed with methanol and deionized (DI) water.

2.3.2. Polar Organic Chemical Integrative Sampler

POCIS enables accumulated concentrations of PFAS to be measured at low concentrations and captures pulses of PFAS in surface waters. The

samplers are composed of two sheets of microporous polyethersulfone membranes encasing a solid phase sorbent (Oasis HLB) to retain the sampled contaminants. Oasis HLB has been used previously to sample PFAS along with other emerging contaminant classes in WWTP and surface water settings (Alvarez et al., 2004, 2008, 2020b; Caniglia et al., 2022; Van Metre et al., 2017).

POCIS and OASIS HLB sorbent membranes were purchased from Environmental Science and Technology (EST) Inc. in Missouri, USA. Each WWTP had four sampling sites: untreated influent, treated effluent, upstream of EMZ, and downstream of EMZ. At each site, one POCIS canister with 2 OASIS HLB membranes were deployed to assess PFAS analytes (Fig. S2). The POCIS were deployed for 14 days during each sampling period. The first sampling period was from April 4–18, 2022, and the second was July 13–27, 2022.

POCIS were secured using $\frac{1}{2}$ inch thick, braided nylon rope, attached to the canister and a nearby permanent fixture (i.e., guard rails, trees, etc.; Fig. S3). POCIS were transported to and from each site in labeled, 2-gallon Ziploc bags to prevent contamination during travel and were transported back to the Messer Water Quality Laboratory at the University of Kentucky (UK) in Lexington, KY in Ziploc bags on ice in a cooler. Once at the lab, any debris was carefully removed before placing each OASIS HLB membrane in individually labeled 6 in x 6 in sealable polypropylene bags. The bagged membranes were placed in a stainless-steel canister and kept in a freezer at -28.8°C until ready to ship for analysis. Light exposure was minimized as much as possible during this process to prevent photodegradation. Four POCIS samples were taken at each monitoring site (2 during the April sampling and 2 during the July sampling). Sampling periods were chosen in order to capture spring flush at the beginning of the growing season (April) and the typically warmest period of the summer (July) in this region.

POCIS samples were sent to the Nebraska Water Sciences Laboratory (WSL) in Lincoln, Nebraska. PFAS analytes were extracted and analyzed using the methods described in Caniglia et al. (2022) and Gobelius et al. (2019). Surrogates were added to POCIS extracts to estimate suppression/enhancement from individual matrices. (see Supplementary material for details). Briefly, POCIS membranes were carefully separated to expose the internal resin, which was funneled with distilled deionized water (DDI) into a polypropylene cartridge outfitted with a 20 mm porosity polyethylene frit. Another frit was added on top of the resin and was dried on a vacuum line. The sample was then spiked with 4 ng of surrogate spike (Cambridge Isotopes Laboratory, Massachusetts, US) and dried again. Finally, the sample was eluted into polypropylene centrifuge tubes with 20 mL of methanol, mixed, and dried with N gas before being brought up in 230 μL of methanol, $\sim 10 \mu\text{L}$ of water, and a final spike of 2 ng internal standard.

Chromatographic separation for PFAS extracts were analyzed using an Acuity-H Class Plus ultrahigh pressure liquid chromatography (UPLC) system with a 1.7 μm Premeir BEH C818 column equipped with a 2.1 Å \sim 50 mm isolator interfaced to a Xevo TQS triple quadrupole mass spectrometer using an UniSprayTM source operating in a negative ion detection mode (Waters Corporation, Milford, MA). Complete instrumentation settings can be found in Table S2. Seven standards ranging from 0 to 20 ng/mL were used to create the instrumental calibration curve. Method detection limits (MDLs) of the water and solid samples were determined using replicate analysis of a low-level fortified matrix (US EPA, 2016). Details for validation can be found in the Supplementary Materials.

Results from the analysis of POCIS extracts led to mass uptake of contaminant (ng/POCIS) for each analyte. Each value was then converted to a time weighted average (TWA) concentration (ng/L) by using the equation below (Ahrens et al., 2015; Caniglia et al., 2022; Gobelius et al., 2019; Ibrahim et al., 2013; Mathon et al., 2022; Noro et al., 2020).

$$\text{TWA concentration} = \frac{\text{mass of extracted analyte}}{\text{Rs} * \text{deployment time}}$$

where the uptake rate, R_s (L/day), was a unique value depending on the analyte (Table S1). Uptake of 2 PFAS precursors (NETFOSAA and NMeFOSAA) and 1 PFCA (PFTDA) were not converted to time weighted average concentrations as these analytes did not have uptake rates determined for POCIS sampling at the time of the study. Uptake results for all analytes (ng/POCIS) can be found in Table S3.

2.3.3. Sediment and biosolids

Fine surficial transient sediment deposits comprised of silt and clay-sized particles, termed the surficial fine-grained laminae (SFGL), are prevalent throughout the Inner-Bluegrass region of central Kentucky and have a high specific surface area for contaminant accumulation (Ford et al., 2017; Ford and Fox, 2014). To collect sediment samples, a 10-inch PVC pipe was pushed as far into the streambed as possible. Then, a small PVC rod was used to agitate the top 5–10 mm of sediment within the 10-inch PVC cylinder, mobilizing the SFGL. Two grab samples were then collected in 1 L HDPE wide-mouth bottles. This process was repeated along three cross sections at the left bank, thalweg, and right bank, moving further upstream with each cross section. Some locations were not possible due to scouring of the stream bed. The sample personnel had well washed, gloved hands, and was always standing downstream of the PVC pipe. Biosolid samples were obtained directly from the WWTP facility and were stored in a 1 L HDPE bottle. Sample bottles were placed in 2-gallon Ziploc bags and kept on ice in a cooler during transport back to the Messer Water Quality Laboratory.

Once at the lab, the sediment samples were stored at 1 °C for 24 h to allow sediment to settle. Samples were then decanted as much as possible before agitating the remaining water/sediment and transferring into 750 mL centrifuge bottles. Samples were repeatedly centrifuged at 3200 RPM for 6 min and decanted until only sediment remained (Sorvall Legend XTR Centrifuge, Thermo Fisher Scientific Inc., Waltham, Massachusetts). All sediment from each stream site was combined to form one homogenous sample per site. Biosolids and decanted sediment samples were placed in labeled Ziploc bags and frozen (−28.8 °C) until ready to ship for analysis at the Nebraska Water Science Laboratory, where solid samples were extracted using methods described in Caniglia et al. (2022) and Rankin et al. (2016). In summary, sediment and biosolids were air dried, crushed into fine homogenous mix, and 5 g were weight into a 15 mL PP tube and spiked with 4 ng of surrogate spike before processing as described by Caniglia et al. (2022).

2.3.4. Supplemental surface water parameters

Grab samples for nutrient analysis (total organic carbon, ammonia, bromide, chloride, nitrate, nitrate-N, orthophosphate, orthophosphate-P, sulfate, total nitrogen, and total phosphorus) were collected at all stream sites during POCIS removal. Total organic carbon (TOC) was analyzed at the Messer Water Quality Laboratory using a TOC-L (Shimadzu Scientific Instruments, Inc., Maryland, USA). All other nutrients were analyzed using ion chromatography on a Dionex ICS-3000 (Thermo-Fisher Scientific, Inc., Massachusetts, USA) at the Kentucky Geologic Survey Facility located on UK's campus (Lexington, KY). Each parameter and the associated method reference can be found in Table S4.

2.4. Mass flow calculations

The total mass, m (mg) and average mass flux, \dot{m}_{water} (mg/day) of contaminants in the WWTP, concentration percent changes, WWTP mass load into downstream surface waters, \dot{m}_{WWTP} (mg/day), mass rate of contaminant removal per day, \dot{m}_{loss} (mg/day), and removal efficiency, $\%m_{loss}$ of each contaminant, were calculated as a function of contaminant concentration, volumetric discharge and deployment time following methods described in Pan et al. (2016) and detailed in the supplementary materials.

2.5. Statistics

Statistical analyses were completed for all PFAS analytes that were detected at more than two locations. When addressing non-detects, values that were less than the minimum detection limit but were still reported were left as is, while values of zero were changed to the lower of either one half of the minimum detection limit or one half of the lowest reported value for that analyte/aqueous compartment. Data was then normalized via natural log transformation. One-way ANOVA/Tukey's honest significant difference (HSD) comparisons were made between location (either upstream/downstream or influent/effluent) and month (April/July) and were stratified by WWTP. T-tests were used to assess differences between the WWTPs. If an analyte did not have a POCIS uptake rate, their mass uptake (ng/POCIS) was used in the statistical analysis instead of concentration. Linear multivariate statistical assessments were completed to assess relationships between monitored water biogeochemical properties and PFAS compounds, subgroups, and totals. Statistical significance was determined at the $\alpha = 0.05$ level; however, all p-values and Tukey's HSD groups can be found in supplementary materials (Tables S5–S7). Statistical analyses were conducted in SAS 9.4 (SAS Institute Inc, North Carolina, USA). Concentrations and standard deviations are reported throughout the results.

3. Results and discussion

3.1. Overall occurrence

3.1.1. Aqueous samples

During the study, 5 to 14 PFAS analytes were detected above the MDL (0.05 ng/POCIS) at each site with concentrations ranging from the MDL to 393 ng/L (Table S8). Overall, short chain PFAS were detected more frequently and had a higher overall average concentration than long chain PFAS. Specifically, short chain PFCAs were detected in 97% of samples (average concentration 17.6 ng/L), while long chain PFCAs were detected in 62% of samples (average concentration 4.41 ng/L). Short chain PFSAs had no difference in detection frequency (DF) compared to long chain PFSAs (both 100%) but did have a higher overall average concentration (33.0 ng/L compared to 23.4 ng/L). Aqueous concentrations were dominated by PFSAs (PFHxS, PFBS, and PFOS) as well as PFOA, a long chain PFCA (Fig. 2), all of which are analytes that have been reported at the highest concentrations when assessing similar suites of PFAS in other studies (Coggan et al., 2019; Sardiña et al., 2019). PFAS precursors were also frequently detected throughout the study (64% DF). Perfluoroalkyl ether acids, which include PFECA's and PFES', were the least detected PFAS group (Table S9), with HFPO-DA being the only analyte in this category to be detected; however, both HFPO-DA detections were below the MDL.

Similar to our observations, previous PFAS studies in WWTPs have observed frequent detection of PFAAs and infrequent or complete lack of detection of PFECA's and PFES' (Campo et al., 2014; Caniglia et al., 2022; Coggan et al., 2019; Guerra et al., 2014). For example, Coggan et al. (2019) reported median detection rates for 17 PFAAs and 2 PFECA's across 19 Australian WWTPs with 96% and 2% detection frequencies, respectively. Frequent observations of PFAAs could be due to well-established analytical methods compared to other PFAS groups, which result in more frequent testing compared to other forms. PFAAs include legacy PFAS, such as PFOA and PFOS, which despite their general phase-out in the United States, still exhibit high environmental accumulation as they do not break down in the environment (US EPA, 2015). Lower DFs of PFECA's and PFES' was likely due to the recent introduction of these forms to the market in an effort to replace long-chain PFAAs, thus leaving less time to accumulate in the environment (Munoz et al., 2019b; Pan et al., 2018; Sun et al., 2016). Analytes also may have transformed into PFAAs prior to reaching the sampling locations in this study (Xiao, 2017). While PFECA's and PFES' were not detected in this study, these forms have been detected in studies in China

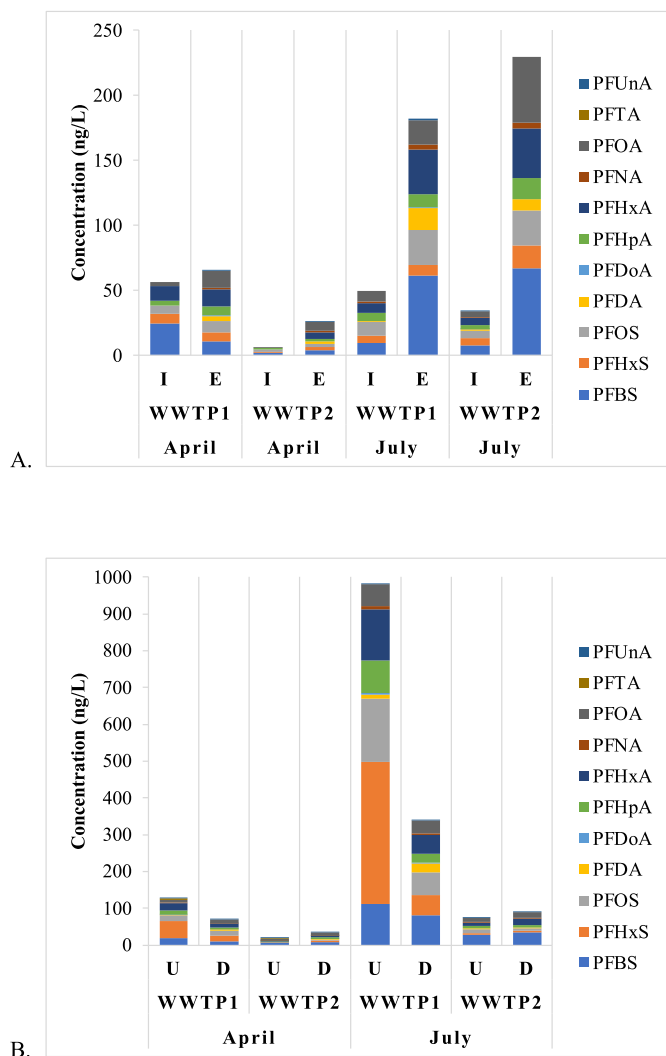


Fig. 2. Cumulative sum of 11 PFAS analytes at the influent (I) and effluent (E) (A) and analytes upstream (U) and downstream (D)(B) of WWTP1 and WWTP2 in April and July.

(Ruan et al., 2015; S. Wang et al., 2013).

WWTP1's upstream site had the highest overall PFAS concentration in both April and July. The notably high concentration of PFHxS at WWTP1's upstream site likely was due to its location downstream of a firefighting training facility. A 2019 study of Eastern United States drinking water wells found proximity to firefighting training facilities as the second most influential predictor variable of PFAS presence (behind tritium) (McMahon et al., 2022). This is because of the aqueous film forming foams (AFFFs) used to fight fires, which are known sources of PFAS into the environment (Cui et al., 2020; Hu et al., 2016).

3.1.2. Sediment and biosolids

In biosolids ($n = 4$), 11 PFAS analytes were detected at least once above the MDL of 0.05 ng/g. In sediment samples ($n = 8$) 12 PFAS analytes were detected at least once above the MDL. For both biosolid and sediment samples, long chain PFSAs were detected at a higher frequency than short chain PFSAs (100% and 29%, respectively) as well as had a higher overall average concentration (1.67 ng/g and 0.06 ng/g, respectively). PFCA detection frequency was similar between long and short chain analytes (36% and 33%, respectively) and overall average concentrations did not differ notably (0.07 ng/g and 0.10 ng/g) (Table S9). It should be noted that PFAS concentrations in biosolids and sediment were dominated heavily by PFOS, which was the only long

chain PFSA assessed in this study (Fig. 3).

The low sediment concentrations in this study were similar to studies of the Yangtze River in China (0.05–1.44 ng/g DW), the Pearl River Delta Region in South China (max concentration 11.4 ng/g DW), the Bohai Sea in China (0.33–2.78 ng/g DW), and France (average concentration 3.0 ± 1.2 ng/g DW), but were lower than some other observations of the Ebro Delta in Spain (1.02–22.6 ng/g DW), and Nevada (max concentration 88.2 ng/g DW) (Bai and Son, 2021; Chen et al., 2016; Munoz et al., 2019a; C. G. Pan et al., 2014b; C. G. Pan et al., 2014a; Pignotti et al., 2017). In biosolids, concentrations were lower than reported concentrations in Australia, which saw maximum concentrations of PFOS reaching 90 ng/g DW (Coggan et al., 2019). Similar to our observations, previous studies reported primarily long-chain

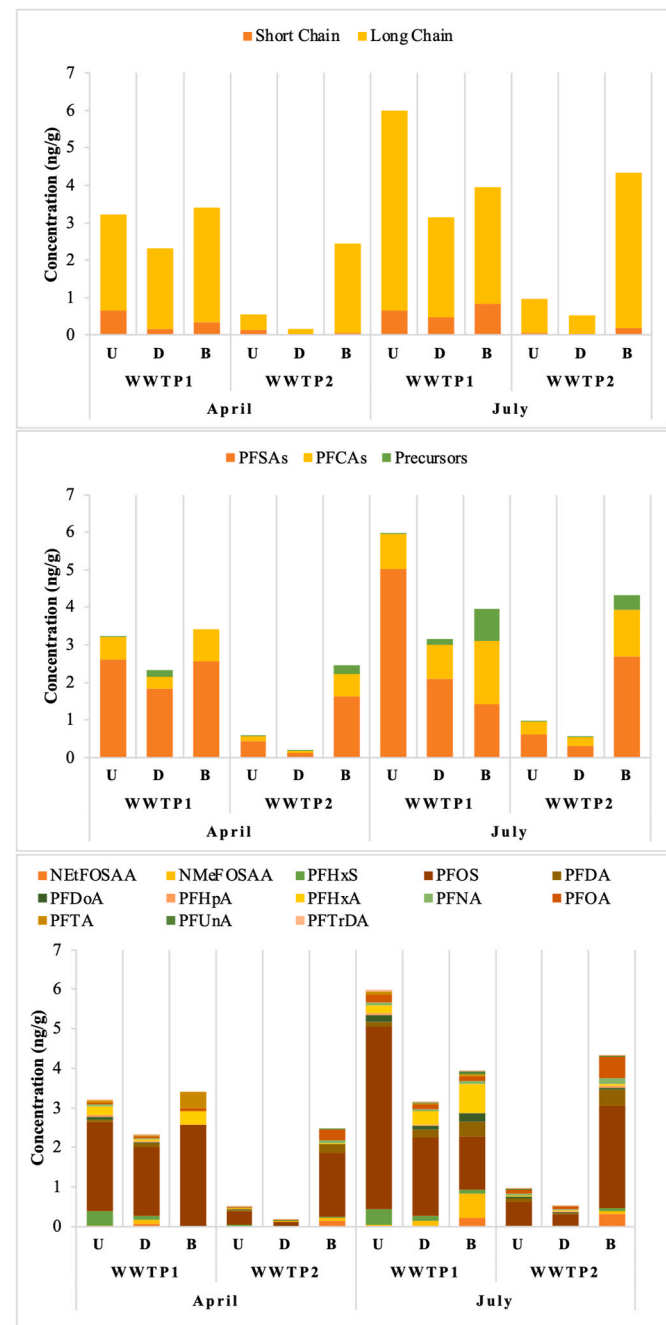


Fig. 3. Sum of PFAS in upstream (U) and downstream (D) sediment and biosolids (B) by chain length (top), PFAS group (middle), and individual analyte (bottom).

PFAS with the highest concentrations being PFOA and PFOS (Chen et al., 2016; Coggan et al., 2019; Munoz et al., 2019a; C. G. Pan et al., 2014a; C. G. Pan et al., 2014b; Pignotti et al., 2017; Rankin et al., 2016). Average PFAS detection frequency above the MDL in sediment and biosolids were slightly lower in April than in July (24% and 37% respectively) (Table S9). Despite the increase in detection frequency in July, concentrations remained relatively low during both sample periods and ranged from <MDL to 4.6 ng/g (Table S10).

3.2. PFAS concentrations

3.2.1. Influent to effluent

Almost every PFAS analyte had significantly higher concentrations ($\alpha = 0.05$) in effluent compared to influent at least once (Fig. 2A). PFOA, PFNA, PFDA, and Σ Long chain PFAS increased the most consistently, followed by PFUNA, PFHxA, PFHpA, Σ PFAS, Σ PFCAs, and Σ Short chain PFAS. Significantly higher effluent concentrations were more common in July (81%) than April (57%) but had similar detection frequencies (WWTP1 with 70% and WWTP2 with 67%).

At WWTP1, the average total (Σ PFAS) dissolved phase TWA concentrations in the influent and effluent for both sampling periods were 53 ± 4.29 ng/L and 124 ± 68.75 ng/L, respectively (Fig. 2A). In April, the sum of PFSAs decreased slightly (-31%), while the sum of PFCAs increased dramatically (118%); however, in July, the sums of PFSAs and PFCAs both increased (274% and 263%, respectively) (Table S11). At WWTP2, average concentrations across both sampling periods for influent and effluent were 20.6 ± 16.39 ng/L and 127.4 ± 125.36 ng/L, respectively (Fig. 2A). The sum of PFSAs and PFCAs increased in April (99% and 659%, respectively) and July (493% and 656%, respectively) at WWTP2.

Wang et al. (2022) observed in a PFAS review across 13 studies of WWTPs that PFCAs tended to increase from influent to effluent while PFSAs tended to remain relatively similar or decrease slightly during the WWTP process. This was attributed to the likelihood of precursors to PFOA (a PFCA) being more reactive to chlorination than the precursors for PFOS (a PFSA) (Xiao et al., 2018). While this study only observed one instance and location of overall PFSA concentrations decreasing from influent to effluent (WWTP1 April), in general, this study observed overall larger percent increases for PFCAs compared to PFSAs. This observation suggests that differences in reactivity may exist between PFCA and PFSA precursors (Zhang et al., 2021). Additionally, the markedly larger percent increases observed in July compared to April suggest factors such as increased temperature and/or bacterial populations further influence PFAS transformation processes (hydrolysis, photolysis, aerobic biotransformation) of both PFSAs and PFCAs precursors (Berhanu et al., 2023; Jiang et al., 2006; Speight, 2018). However, due to low sample size, conclusions regarding the factors influencing the differences in PFCA and PFSA transformations could not be drawn; however, the observations from this study indicate PFAS transformation drivers in WWTPs, particularly variability in PFSAs is one that requires further research.

Increases in the sum of PFAS from influent to effluent of WWTPs were similar to past studies. Caniglia et al. (2022) observed TWA concentrations increased from 27.9 ng/L in influent to 132 ng/L in effluent at a WWTP in Nebraska. Similarly, Coggan et al. (2019) observed mean PFAS concentrations increase from 76 ng/L in influent to 140 ng/L in effluent across 19 WWTPs in Australia. In all cases, increases from influent to effluent were attributed to degradation of PFAS precursors into terminal PFAS, typically PFAAs.

3.2.2. Upstream to downstream (aqueous samples)

At WWTP1, the Σ PFAS dissolved phase TWA concentrations at the upstream and downstream sites across both sampling periods were 556.1 ± 493.84 ng/L and 205.0 ± 158.79 ng/L, respectively (Fig. 2B). Every analyte except PFOA and PFNA differed significantly ($\alpha = 0.05$) between upstream and downstream at least once (Fig. S4). PFHxS,

PFHxA, PFHpA, PFDoA, Σ PFAS, Σ PFSAs, Σ PFCAs, and Σ Short chain concentrations decreased from upstream to downstream in both April and July. PFBS, PFUnA, PFTrDA, and PFOS concentrations decreased from upstream to downstream in either April or July. In contrast, Σ Precursors NMeFOSAA, and NEtFOSAA increased significantly from upstream to downstream in April and July.

At WWTP2, Σ PFAS dissolved phase TWA concentrations at the upstream and downstream sites across both sampling periods were 47.0 ± 31.7 ng/L and 62.3 ± 31.1 ng/L (Fig. 2B). Every analyte except PFDA and NEtFOSAA differed significantly ($\alpha = 0.05$) between upstream and downstream at least once (Fig. S4). Most PFAS analytes and groups exhibiting significant changes were higher downstream of the EMZ, excluding PFuNA, PFDoA, PFTrDA, NMeFOSAA, and Σ Precursors, which were higher upstream of the EMZ when significant.

Differences in trends observed between studies and within our study may be due to differing PFAS sources. Few studies have compared upstream to downstream concentrations of PFAS surrounding WWTPs. Caniglia et al. (2022) observed an increase in concentration from upstream to downstream for 12 of 14 detected PFAS analytes analyzing one WWTP in Eastern Nebraska. In some cases of our study, concentrations were lower at the downstream sites compared to the upstream sites even though concentrations increased from influent to effluent. This was likely due to upstream practices that could have potentially introduced PFAS to the stream via runoff. Thus, the WWTP effluent concentrations, while higher than the influent, were still diluting the upstream concentrations. WWTP1 was located downstream of a firefighting training facility, which are identified sources of PFAS into the environment due to their aqueous film forming foams (AFFF) (Gharehveran et al., 2022; Leeson et al., 2021; Mussabek et al., 2023; Reinikainen et al., 2022). Thus, PFAS analytes primarily originating from the firefighting training facility were likely being diluted by WWTP1 effluent, decreasing from upstream to downstream, while analytes primarily originating from the WWTP, i.e., PFAS precursors/transformation products, were increasing from upstream to downstream. WWTP2 did not have an identified additional source of PFAS into the upstream environment.

3.2.3. Upstream to downstream (sediment samples)

PFAS concentrations in upstream sediment samples were consistently higher than in downstream sediment, even when downstream aqueous concentrations were greater than upstream concentrations (Fig. 3). Altered biogeochemical surface water properties observed downstream of WWTPs may have led to this. Chloride, sulfate, and TOC have been observed to compete with PFAS during sorption to sediment (Kothawala et al., 2017; McMahon et al., 2022). Individual PFAS compounds in this study, Σ long and short chain PFAS, and overall PFAS concentrations, had weak correlations with TOC, pH, NH₄-N, NO₃-N, PO₄-P, TN, sulfate, and TOC ($R^2 = <0.50$). In contrast, strong correlations were observed between increasing aqueous chloride concentrations and increasing PFAS sorption to sediment ($R^2_{PFOS} = 0.75$; $R^2_{PFDoA} = 0.69$; $R^2_{PFHxA} = 0.51$; $R^2_{PFTrDA} = 0.60$; $R^2_{\Sigma Long} = 0.749$; $R^2_{\Sigma Overall} = 0.72$), which is contradictory to past observations (Tables S10–S11). However, due to the low sample size (one sediment collection per site per sampling period) statistical analyses were not able to be completed for sediment samples. However, the results demonstrate a need for further investigation into unique biogeochemical parameters found downstream of WWTPs that may influence PFAS sorption to sediment.

3.2.4. Sampling period differences

When considering wastewater samples (influent and effluent), WWTP2 was impacted more by the sampling period than WWTP1. WWTP2 had significantly higher concentrations in July ($\alpha = 0.05$) for PFOS, PFHxS, PFHpA, PFBS, NEtFOSAA, Σ PFAS, Σ PFSAs, Σ Short chain PFAS, and Σ PFAS precursors, while WWTP1 had no significant differences between April and July. One potential explanation is that WWTP2 was influenced more by rainfall than WWTP1. For example, WWTP1 had a holding tank on site for supplemental water that would be treated

when inflow was low, whereas inflow was nearly stagnant at WWTP2 during POCIS removal in April due to low recent rainfall (Table S13). However, multiple years of testing would be required to confirm this trend.

Surface water samples (upstream and downstream), at both WWTP1 and WWTP2, were impacted by sampling period. At WWTP1, 10 analytes (every detected analyte except PFHxS and NMeFOSAA) were significantly higher ($\alpha = 0.05$) in July than April. At WWTP2, two analytes were higher in April (PFDoA and PFTrDA, the latter of which was only detected in April). Four analytes had no significant difference between April and July (PFUNA, PFOA, NMeFOSAA and NNetFOSAA). The remaining 8 analytes were higher in July.

In part, at WWTP1 these differences were mostly due to variability in contributions of effluent vs. upstream stream flow. During April downstream stream flow was dominated by WWTP1 effluent. In contrast during July, the downstream monitoring station was dominated by upstream contributions. WWTP2 was more inconclusive.

Several biogeochemical characteristics have been found to affect PFAS sorption including granular active carbon, DOC, divalent cations, pH, and chloride (Barth et al., 2021; Crone et al., 2019; Kothawala et al., 2017; McMahon et al., 2022). However, individual PFAS compounds and groups had weak correlations with DOC, pH, $\text{NH}_4\text{-N}$, $\text{NO}_3\text{-N}$, $\text{PO}_4\text{-P}$, TN, sulfate, and TOC ($R^2 = <0.50$) in aqueous samples of this study (Table S12). In contrast, strong, correlations were observed between increasing chloride concentrations and increasing individual PFAS compounds ($R^2 = 0.57$ for PFBS to 0.79 for PFOS), PFAS group ($R^2_{\text{PFSA}} = 0.74$; $R^2_{\text{PFCA}} = 0.75$), \sum long chain ($R^2_{\text{long}} = 0.77$) and \sum short chain ($R^2_{\text{short}} = 0.73$) PFAS, and overall PFAS ($R^2 = 0.75$) in stream samples. Chloride has been found to impact degradation rates of PFAS compounds. For example, PFOA degradation rates have been observed to reduce significantly with increasing chloride concentrations resulting in higher PFOA concentrations, particularly at higher temperatures (Lee et al., 2012), which was similar to observations in this study ($R^2_{\text{PFOA}} = 0.72$).

However, increase in POCIS uptake of NNetFOSAA in July of this study could indicate increased PFAS transformation in July, potentially due to amplified microbial activities with higher temperatures (Guerra et al., 2014). NNetFOSAA is an intermediate product in the breakdown of electrochemical fluorination-based surfactants and polymers into PFOS and PFOA as a result of several degradation pathways, including hydrolysis, photolysis, or aerobic microbial biodegradation which can be impacted by pH and temperature (ITRC (Interstate Technology & Regulatory Council), 2020; Martin et al., 2010). All available temperature and pH data provided by the WWTPs or collected at the surface water sites, as well as other supplementary water quality data can be found in Table S13.

Ideally, samples would have been taken monthly throughout the year to assess seasonality. However, in this study samples were only taken in April (spring period at the monitoring locations) and July (summer period at the monitoring locations). Other studies have shown seasonal patterns of PFAS concentrations vary depending on analyte and region. In North China, the dry season (winter/spring) had significantly higher levels of PFAS contamination in sea water compared to the wet season (summer/fall); however, PFOS exhibited an alternate trend, with concentrations lowest in winter and highest in spring (Han et al., 2020). The Yangtze River in China, however, showed no significant seasonal variation from winter to summer for most PFAS in sediment, but did observe significant differences in water samples seasonally (Pan et al., 2014a). In comparison, the River Elbe in Germany had the highest concentrations of PFOA and PFHxA in August with a potential difference being due to water discharge in the studied river (Zhao et al., 2015). In the United States, a Las Vegas study observed significantly higher concentrations of PFAS in winter compared to summer (Bai and Son, 2021). The lack of consensus regarding the sampling period of PFAS contamination requires further research to understand. Seasonal trends may depend on each region's unique hydrology, climate, and PFAS sources as was

observed in this study.

3.2.5. Wastewater treatment plant comparison

PFAS concentrations were significantly higher ($\alpha = 0.05$) at WWTP1 compared to WWTP2 for PFOS, PFHxS, PFHxA, PFHpA, PFDoA, PFBS, NMeFOSAA, Σ PFAS, Σ PFSA, Σ PFCA, Σ Long chain PFAS, Σ Short chain PFAS, and Σ PFAS precursors. PFUNA, PFOA, PFNA, PFDA, and NNetFOSAA were also significantly higher ($\alpha = 0.05$) at WWTP1 when considering upstream and downstream samples, but not when influent and effluent samples were also considered. These results agree with Sardiña et al. (2019), who sampled soil, sediment, and surface water and found residential and industrial areas had higher PFAS levels than undisturbed and agricultural areas, although the differences in Sardiña's study were not determined to be statistically significant. Urban and industrial areas typically have higher populations than rural, agricultural, and undisturbed areas. This provides more opportunity for the production, use, and disposal of PFAS laden products and while both plants in our study received industrial inputs, WWTP1 was located in a larger, more urbanized city than WWTP2.

3.3. Mass balance and WWTP contribution to the downstream environment

The mass balance of PFAS indicated higher load (mg/day) of the measured PFAS analytes exiting the WWTPs than entering the WWTPs for most analytes. At WWTP1, an additional load of 346.5 and 7411.5 mg/day of PFAS were discharged through effluent and biosolids in April and July, respectively. 98% of the excess PFAS was discharged through effluent and only 2% were in biosolids. Biosolid PFAS concentrations were overall low (3.41–3.96 ng/g) and dominated by PFOS. At WWTP2, an additional 428 and 2860 mg/day of PFAS were discharged in April and July, respectively. In April, the ratio of PFAS discharged in effluent and biosolids was 86:14 while in July it was 97:3. Similarly, biosolid PFAS concentrations were overall low (1.62–2.68 ng/g) and were once again dominated by PFOS. These mass fluxes out of WWTP effluent were similar to a study in Nebraska, which estimated a mass flux of 11,100 mg/day leaving a WWTP into downstream surface waters; however, instantaneous mass load of PFAS in WWTP effluent is not frequently assessed in the literature and this area needs further research (Caniglia et al., 2022). Mass flow rate of each analyte by WWTP and season can be found in Figs. S5 and S6.

3.4. Eco- and human toxicity concerns

Currently, the EPA has draft aquatic life ambient water quality criteria for PFOA and PFOS. The acute benchmarks are 49 mg/L and 3.0 mg/L, respectively and the chronic benchmarks are 0.094 mg/L and 0.0084 mg/L, respectively (United States Environmental Protection Agency, 2022). Research is ongoing to understand the mechanisms of toxicity for these compounds, but impacts on aquatic organism survivability, growth, and reproduction have been observed (United States Environmental Protection Agency, 2022). While these limits were not surpassed by the PFAS observed in this study, it is important to note that the limits are set for only two of many analytes and do not consider the impact of multiple PFAS analytes being in the water at once.

Of more concern are the recent EPA maximum contaminant levels (MCLs) and hazard indexes (HIs) for drinking water. The current MCLs for PFOA and PFOS are 4.0 ng/L. PFOA and PFOS exceeded the recommended limits in this study 81 and 75% of the time (Fig. 4). The proposed HI for the combined concentrations of HFPO-DA, PFBS, PFNA, and PFHxS is 1 (unitless) (U.S. Environmental Protection Agency, 2024). The HI is calculated based off the observed concentrations in water and EPA determined health-based water concentrations (HBWCs) for each analyte using the equation below:

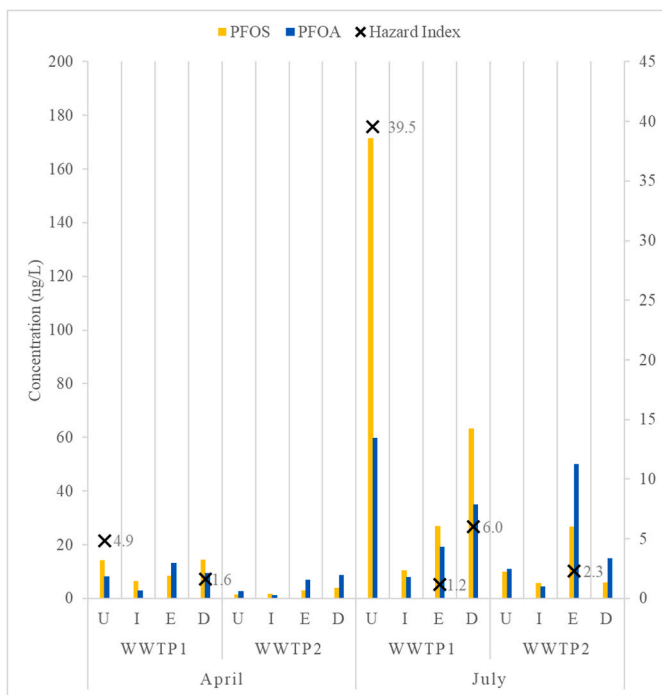


Fig. 4. TWA concentrations (ng/L) of PFOA and PFOS for each upstream (U), downstream (D), influent (I), and effluent (E) site. Hazard index (HI) is shown at sites that exceeded the recommended limit of 1. HI value is shown in parentheses.

$$HI = \frac{HFPO - DA_{water}}{HFPO - DA_{HBWC}} + \frac{PFBS_{water}}{PFBS_{HBWC}} + \frac{PFNA_{water}}{PFNA_{HBWC}} + \frac{PFHxS_{water}}{PFHxS_{HBWC}}$$

where $HFPO - DA_{HBWC} = 10 \text{ ng/L}$, $PFBS_{HBWC} = 2000 \text{ ng/L}$, $PFNA_{HBWC} = 10 \text{ ng/L}$, and $PFHxS_{HBWC} = 10 \text{ ng/L}$ (U.S. Environmental Protection Agency Office of Water, 2024). According to this equation, the HI was exceeded at WWTP1 upstream (4.85–39.5) and downstream (1.6–6.02) in April and July and effluent of WWTP1 (1.2) and WWTP2 (2.3) in July (Fig. 4).

It is important to note the water tested in this study was not intended for human consumption; however, in the Central Kentucky region, surface water is eventually brought into drinking water treatment plants (DWTPs), treated, and distributed throughout the city. For example, the stream that WWTP2 discharges into serves as the primary drinking water for a city approximately 16 km downstream of the WWTP2 effluent discharge point. DWTPs have been more effective at removing PFAS than WWTPs; however, the current recommended drinking water limits were still exceeded post DWTP in Kentucky in 2019 (Department for Environmental Protection, 2019). Thus, the PFAS load being discharged by WWTPs into the downstream aquatic environment could put an increasing strain on DWTPs if the EPA recommended drinking water limits become enforceable.

4. Conclusion

PFAS were detected more frequently in aqueous samples than sediment or biosolids and were primarily discharged from the WWTPs as treated effluent rather than in biosolids. Samples were dominated by PFAAs, primarily PFHxS, PFHxA, PFBS, PFOA, and PFOS. PFHxS was particularly prominent at WWTP1's upstream site, which was attributed to the firefighting training facility located upstream of the sampling location. PFBS was prominent at WWTP2, marking the shift from legacy, long chain PFAS to novel, short chain PFAS. Nearly all measured PFAS persisted in aqueous (86–98%) compartments rather than sediment or biosolids (2–14%).

Effluent concentrations were generally greater than influent concentrations, with significant differences observed more in July than in April. Trends in PFAS increase from influent to effluent were similar between WWTPs even though the WWTPs had varying treatment processes. The WWTPs likely acted as the primary source of PFAS analytes into the downstream environment when that analyte significantly increased from upstream to downstream of the EMZ (i.e., in the case of the PFAS transformation product NEtFOSAA). However, analytes that decreased from upstream to downstream of the EMZ likely had other primary sources into the environment (i.e., the firefighting training facility), resulting in dilution downstream of the EMZ despite overall concentrations increasing within the WWTP. The chemical composition of aqueous film forming foams used to fight fires is rarely disclosed; therefore, it was difficult to confirm the original sources of PFAS observed in the environment.

Finally, there were many occurrences of PFAS exceeding the EPA drinking water limits for PFOA, PFOS, and the combination of PFHxS, PFBS, PFNA and HFPO-DA (GenX), although HFPO-DA was rarely detected in this study. While effluent water is not regulated for PFAS, in surface water dependent regions upstream contributions of PFAS have the potential to increase stress on downstream water treatment facilities using these waters as drinking water sources. Based on recent EPA proposed maximum contaminant levels, hazard indexes for drinking water were exceeded at WWTP1 upstream (5.4–43.8) and downstream (1.8–6.6) in April and July and effluent of WWTP1 (1.2) and WWTP2 (2.5) in July. Future work is needed to explore specific transformation processes for PFAS in WWTPs. Further, WWTPs and land use practices should be considered as increased strains on downstream drinking water source waters in regions that are surface water dependent and downstream ecosystems.

Funding

This material is based upon work supported by the United States (U.S.) Geological Survey under a 104(b) project. The views and conclusions contained in this document are those of the authors and should not be interpreted as representing the opinions of policies of the U.S. Geological Survey. Mention of trade names or commercial products does not constitute their endorsement by the U.S. Geological Survey. This material is also based upon work supported by the National Science Foundation under Grant No. 1922694. This project was also supported with funds by the U.S. Hatch multistate capacity funding grant (W-4045). Any opinions, findings, conclusions, or recommendations expressed in this publication are those of the authors and do not necessarily reflect the view of the U.S. Department of Agriculture and National Science Foundation. Any use of trade, firm, or product names is for descriptive purposes only and does not imply endorsement by the U.S. Government.

CRediT authorship contribution statement

Kyra Sigler: Writing – original draft, Visualization, Validation, Formal analysis, Data curation. **Tiffany L. Messer:** Writing – review & editing, Supervision, Resources, Project administration, Methodology, Funding acquisition, Formal analysis, Conceptualization. **William Ford:** Writing – review & editing, Resources, Funding acquisition. **Wayne Sanderson:** Writing – review & editing, Validation, Methodology.

Declaration of competing interest

The authors declare the following financial interests/personal relationships which may be considered as potential competing interests: Tiffany Messer reports administrative support, equipment, drugs, or supplies, statistical analysis, and travel were provided by United States Geological Survey, U.S. Department of Agriculture, and National Science Foundation. If there are other authors, they declare that they have no known competing financial interests or personal relationships that

could have appeared to influence the work reported in this paper.

Appendix A. Supplementary data

Supplementary data to this article can be found online at <https://doi.org/10.1016/j.jenvman.2024.123129>.

Data availability

I have shared my data as a link in the submission.

References

Ahrens, L., Daneshvar, A., Lau, A.E., Kreuger, J., 2015. Characterization of five passive sampling devices for monitoring of pesticides in water. *J. Chromatogr. A* 1405. <https://doi.org/10.1016/j.chroma.2015.05.044>.

Alvarez, D.A., Cranor, W.L., Perkins, S.D., Clark, R.C., Smith, S.B., 2008. Chemical and toxicologic assessment of organic contaminants in surface water using passive samplers. *J. Environ. Qual.* 37, 1024–1033. <https://doi.org/10.2134/jeq2006.0463>.

Alvarez, D.A., Petty, J.D., Huckins, J.N., Jones-Lepp, T.L., Getting, D.T., Goddard, J.P., Manahan, S.E., 2004. Development of a passive, in situ, integrative sampler for hydrophilic organic contaminants in aquatic environments. *Environ. Toxicol. Chem.* 23, 1640–1648. <https://doi.org/10.1897/03-603>.

Bai, X., Son, Y., 2021. Perfluoroalkyl substances (PFAS) in surface water and sediments from two urban watersheds in Nevada, USA. *Sci. Total Environ.* 751. <https://doi.org/10.1016/j.scitotenv.2020.141622>.

Barth, E., KcKernan, J., Bless, D., Dasu, K., 2021. Investigation of an immobilization process for PFAS contaminated soils. *J. Environ. Manag.* 296. <https://doi.org/10.1016/j.jenvman.2021.113069>.

Bao, J., Yu, W.J., Liu, Y., Wang, X., Jin, Y.H., Dong, G.H., 2019. Perfluoroalkyl substances in groundwater and home-produced vegetables and eggs around a fluorochemical industrial park in China. *Ecotoxicol. Environ. Saf.* 171. <https://doi.org/10.1016/j.ecoenv.2018.12.086>.

Beni, N.N., Snow, D.D., Berry, E.D., Mittelstet, A.R., Messer, T.L., Bartelt-Hunt, S., 2020. Measuring the occurrence of antibiotics in surface water adjacent to cattle grazing areas using passive samplers. *Sci. Total Environ.* 726, 138296. <https://doi.org/10.1016/j.scitotenv.2020.138296>.

Berhanu, A., Mutanda, I., Taolin, J., Qaria, M.A., Yang, B., Zhu, D., 2023. A review of microbial degradation of per- and polyfluoroalkyl substances (PFAS): biotransformation routes and enzymes. *Sci. Total Environ.* 859, 160010. <https://doi.org/10.1016/j.scitotenv.2022.160010>.

Brase, R.A., Mullin, E.J., Spink, D.C., 2021. Legacy and emerging per- and polyfluoroalkyl substances: analytical techniques, environmental fate, and health effects. *Int. J. Mol. Sci.* 22 (3). <https://doi.org/10.3390/ijms22030995>.

Buck, R.C., Franklin, J., Berger, U., Conder, J.M., Cousins, I.T., Voogt, P.D., Jensen, A.A., Kannan, K., Mabury, S.A., van Leeuwen, S.P.J., 2011. Perfluoroalkyl and polyfluoroalkyl substances in the environment: terminology, classification, and origins. *Integrated Environ. Assess. Manag.* 7 (4), 513–541. <https://doi.org/10.1002/IEAM.258>.

Campo, J., Masiá, A., Picó, Y., Farré, M., Barceló, D., 2014. Distribution and fate of perfluoroalkyl substances in Mediterranean Spanish sewage treatment plants. *Sci. Total Environ.* 472. <https://doi.org/10.1016/j.scitotenv.2013.11.056>.

Caniglia, J., Snow, D.D., Messer, T., Bartelt-Hunt, S., 2022. Extraction, analysis, and occurrence of per- and polyfluoroalkyl substances (PFAS) in wastewater and after municipal biosolids land application to determine agricultural loading. *Frontiers in Water.* <https://doi.org/10.3389/frwa.2022.892451>.

Chen, H., Sun, R., Zhang, C., Han, J., Wang, X., Han, G., He, X., 2016. Occurrence, spatial and temporal distributions of perfluoroalkyl substances in wastewater, seawater and sediment from Bohai Sea, China. *Environmental Pollution (Barking, Essex : 1987)* 219. <https://doi.org/10.1016/j.envpol.2016.05.017>.

Coggan, T.L., Moodie, D., Kolobaric, A., Szabo, D., Shimeta, J., Crosbie, N.D., Lee, E., Fernandes, M., Clarke, B.O., 2019. An investigation into per- and polyfluoroalkyl substances (PFAS) in nineteen Australian wastewater treatment plants (WWTPs). *Helijon* 5 (8), e02316. <https://doi.org/10.1016/J.HELJON.2019.E02316>.

Crone, B.C., Speth, T.F., Wahman, D.G., Smith, S.J., Abulikemu, G., Kleiner, E.J., Pressman, J.G., 2019. Occurrence of per- and polyfluoroalkyl substances (PFAS) in source water and their treatment in drinking water. *Crit. Rev. Environ. Sci. Technol.* 49 (24), 2359–2396. <https://doi.org/10.1080/10643389.2019.1614848>.

Cui, D., Li, X., Quinete, N., 2020. Occurrence, fate, sources and toxicity of PFAS: what we know so far in Florida and major gaps. *TrAC, Trends Anal. Chem.* 130, 115976. <https://doi.org/10.1016/J.TRAC.2020.115976>.

Dalahmeh, S., Tigrani, S., Komakech, A.J., Niwagaba, C.B., Ahrens, L., 2018. Per- and polyfluoroalkyl substances (PFASs) in water, soil and plants in wetlands and agricultural areas in Kampala, Uganda. *Sci. Total Environ.* 631–632, 660–667. <https://doi.org/10.1016/J.SCITOTENV.2018.03.024>.

Department for Environmental Protection, 2019. Evaluation of Kentucky Community Drinking Water for Per- & Poly-Fluoroalkyl Substances. D. of W.

Flynn, R.W., Hoskins, T.D., Iacchetta, M., de Perre, C., Lee, L.S., Hoverman, J.T., Sepulveda, M.S., 2021. Dietary exposure and accumulation of per- and polyfluoroalkyl substances alters growth and reduces body condition of post-metamorphic salamanders. *Sci. Total Environ.* 765, 142730. <https://doi.org/10.1016/J.SCITOTENV.2020.142730>.

Ford, W.I., Fox, J.F., 2014. Benthic control on the statistical distribution of transported sediment carbon in a low-gradient stream. *J. Hydrol.* 515. <https://doi.org/10.1016/j.jhydrol.2014.05.012>.

Ford, W.I., Fox, J.F., Pollock, E., 2017. Reducing equifinality using isotopes in a process-based stream nitrogen model highlights the flux of algal nitrogen from agricultural streams. *Water Resour. Res.* 53 (8). <https://doi.org/10.1002/2017WR020607>.

Ghareveran, M.M., Walus, A.M., Anderson, T.A., Subbiah, S., Guelfo, J., Frigon, M., Longwell, A., Suski, J.G., 2022. Per- and polyfluoroalkyl substances (PFAS)-free aqueous film forming foam formulations: chemical composition and biodegradation in an aerobic environment. *J. Environ. Chem. Eng.* 10 (6). <https://doi.org/10.1016/j.jece.2022.108953>.

Gobelius, L., Persson, C., Wiberg, K., Ahrens, L., 2019. Calibration and application of passive sampling for per- and polyfluoroalkyl substances in a drinking water treatment plant. *J. Hazard Mater.* 362. <https://doi.org/10.1016/j.jhazmat.2018.09.005>.

Goodrow, S.M., Ruppel, B., Lippincott, R.L., Post, G.B., Procopio, N.A., 2020. Investigation of levels of perfluoroalkyl substances in surface water, sediment and fish tissue in New Jersey, USA. *Sci. Total Environ.* 729. <https://doi.org/10.1016/j.scitotenv.2020.138839>.

Guerra, P., Kim, M., Kinsman, L., Ng, T., Alaei, M., Smyth, S.A., 2014. Parameters affecting the formation of perfluoroalkyl acids during wastewater treatment. *J. Hazard Mater.* 272. <https://doi.org/10.1016/j.jhazmat.2014.03.016>.

Hamid, H., Li, L.Y., 2016. Role of wastewater treatment plant in environmental cycling of poly- and perfluoroalkyl substances. *Ecocycles* 2 (2), 43–53. <https://doi.org/10.19040/ECOCYCLES.V2I2.62>.

Han, T., Gao, L., Chen, J., He, X., Wang, B., 2020. Spatiotemporal variations, sources and health risk assessment of perfluoroalkyl substances in a temperate bay adjacent to metropolis, North China. *Environmental Pollution* 265. <https://doi.org/10.1016/j.envpol.2020.115011>.

Hu, X.C., Andrews, D.Q., Lindstrom, A.B., Bruton, T.A., Schaider, L.A., Grandjean, P., Lohmann, R., Carignan, C.C., Blum, A., Balan, S.A., Higgins, C.P., Sunderland, E.M., 2016. Detection of poly- and perfluoroalkyl substances (PFASs) in U.S. Drinking water linked to industrial sites, military fire training areas, and wastewater treatment plants. *Environ. Sci. Technol. Lett.* 3 (10), 344–350. <https://doi.org/10.1021/acs.estlett.6b00260>.

Ibrahim, I., Togola, A., Gonzalez, C., 2013. Polar organic chemical integrative sampler (POCIS) uptake rates for 17 polar pesticides and degradation products: Laboratory calibration. *Environ. Sci. Pollut. Control Ser.* 20 (6). <https://doi.org/10.1007/s11356-012-1284-3>.

ITRC (Interstate Technology & Regulatory Council), 2020. History and use of per- and polyfluoroalkyl substances (PFAS) found in the environment. <https://pfas-1.itrcweb.org/>.

Jiang, H., Zheng, Z., Li, Z., Wang, X., 2006. Effects of temperature and solvent on the hydrolysis of alkoxysilane under alkaline conditions. *Ind. Eng. Chem. Res.* 45 (25), 8617–8622. <https://doi.org/10.1021/ie0607550>.

Kentucky Infrastructure Authority Office of the Governor, 2021. WRIS system data report KY0021491—LFUCC - town branch. <http://www.lexingtonky.gov/index.aspx?page=665>.

Kentucky Infrastructure Authority Office of the Governor, 2022. WRIS System Data Report KY0037991—Winchester Municipal Utilities.

Kirk, M., Smurthwaite, K., Bräunig, J., Trevenar, S., Lucas, R., Lal, A., Korda, R., Clements, A., Mueller, J., Armstrong, B.P., 2018. The PFAS Health Study Systematic Literature Review. The Australian National University, Canberra. <http://nceph.anu.edu.au/>.

Koch, A., Jonsson, M., Yeung, L.W.Y., Kärrman, A., Ahrens, L., Ekblad, A., Wang, T., 2020. Per- and polyfluoroalkyl-contaminated freshwater impacts adjacent riparian food webs. *Environ. Sci. Technol.* 54 (19), 11951–11960. https://doi.org/10.1021/ACS.EST.0C01640/SUPPL_FILE/ESOC01640_SI_001.PDF.

Kothawala, D.N., Köhler, S.J., Östlund, A., Wiberg, K., Ahrens, L., 2017. Influence of dissolved organic matter concentration and composition on the removal efficiency of perfluoroalkyl substances (PFASs) during drinking water treatment. *Water Res.* 121. <https://doi.org/10.1016/j.watres.2017.05.047>.

Kwiatkowski, C.F., Andrews, D.Q., Birnbaum, L.S., Bruton, T.A., Dewitt, J.C., Knappe, D.R.U., Maffini, M.V., Miller, M.F., Pelch, K.E., Reade, A., Soehl, A., Trier, X., Venier, M., Wagner, C.C., Wang, Z., Blum, A., 2020. Scientific basis for managing PFAS as a chemical class. *Environ. Sci. Technol. Lett.* 7, 532–543. <https://doi.org/10.1021/acs.estlett.0c00255>.

Lee, Y., Lo, S., Kuo, J., Hsieh, 2012. Decomposition of perfluorooctanoic acid by microwaveactivated persulfate: effects of temperature, pH, and chloride ions. *Front. Environ. Sci. Eng.* 6, 17–25.

Leeson, A., Thompson, T., Stroo, H.F., Anderson, R.H., Speicher, J., Mills, M.A., Willey, J., Coyle, C., Ghosh, R., Lebrón, C., Patton, C., 2021. Identifying and managing aqueous film-forming foam-derived per- and polyfluoroalkyl substances in the environment. *Environ. Toxicol. Chem.* 40 (1). <https://doi.org/10.1002/etc.4894>.

Lenka, S.P., Kah, M., Padhye, L.P., 2021. A review of the occurrence, transformation, and removal of poly- and perfluoroalkyl substances (PFAS) in wastewater treatment plants. *Water Res.* 199. <https://doi.org/10.1016/j.watres.2021.117187>.

Martin, J.W., Asher, B.J., Beeson, S., Benskin, J.P., Ross, M.S., 2010. PFOS or PreFOs? Are perfluorooctane sulfonate precursors (PreFOs) important determinants of human and environmental perfluorooctane sulfonate (PFOS) exposure? *J. Environ. Monit.* 12 (11). <https://doi.org/10.1039/c0em00295j>.

Masner, J.R., Kolpin, D.W., Cozzarelli, I.M., Smalling, K.L., Bolyard, S.C., Field, J.A., Furlong, E.T., Gray, J.L., Lozinski, D., Reinhart, D., Rodowa, A., Bradley, P.M., 2020. Landfill leachate contributes per-/poly-fluoroalkyl substances (PFAS) and pharmaceuticals to municipal wastewater. *Environmental Science: Water Research and Technology* 6 (5). <https://doi.org/10.1039/d0ew00045k>.

Mathon, B., Ferreol, M., Togola, A., Lardy-Fontan, S., Dabrin, A., Allan, I.J., Staub, P.F., Mazzella, N., Miège, C., 2022. Polar organic chemical integrative samplers as an effective tool for chemical monitoring of surface waters – results from one-year monitoring in France. *Sci. Total Environ.* 824. <https://doi.org/10.1016/j.scitotenv.2022.153549>.

McMahon, P.B., Tokranov, A.K., Bexfield, L.M., Lindsey, B.D., Johnson, T.D., Lombard, M.A., Watson, E., 2022. Perfluoroalkyl and polyfluoroalkyl substances in groundwater used as a source of drinking water in the eastern United States. *Environ. Sci. Technol.* 56 (4). <https://doi.org/10.1021/acs.est.1c04795>.

Munoz, G., Budzinski, H., Babut, M., Lobry, J., Selleslagh, J., Tapie, N., Labadie, P., 2019a. Temporal variations of perfluoroalkyl substances partitioning between surface water, suspended sediment, and biota in a macrotidal estuary. *Chemosphere* 233. <https://doi.org/10.1016/j.chemosphere.2019.05.281>.

Munoz, G., Liu, J., Vo Duy, S., Sauvé, S., 2019b. Analysis of F-53B, Gen-X, ADONA, and emerging fluoroalkylether substances in environmental and biomonitoring samples: a review. *Trends in Environmental Analytical Chemistry* 23, e00066. <https://doi.org/10.1016/j.teac.2019.e00066>.

Mussabek, D., Söderman, A., Imura, T., Persson, K.M., Nakagawa, K., Ahrens, L., Berndtsson, R., 2023. PFAS in the drinking water source: analysis of the contamination levels, origin and emission rates. *Water (Switzerland)* 15 (1). <https://doi.org/10.3390/w15010137>.

Noro, K., Endo, S., Shikano, Y., Banno, A., Yabuki, Y., 2020. Development and calibration of the polar organic chemical integrative sampler (POCIS) for neonicotinoid pesticides. *Environ. Toxicol. Chem.* 39 (7). <https://doi.org/10.1002/etc.4729>.

Olsen, G.W., 2015. PFAS biomonitoring in higher exposed populations. *Molecular and Integrative Toxicology* 77–125. https://doi.org/10.1007/978-3-319-15518-0_4.

Pan, C.G., Liu, Y.S., Ying, G.G., 2016. Perfluoroalkyl substances (PFASs) in wastewater treatment plants and drinking water treatment plants: removal efficiency and exposure risk. *Water Res.* 106. <https://doi.org/10.1016/j.watres.2016.10.045>.

Pan, C.G., Ying, G.G., Liu, Y.S., Zhang, Q.Q., Chen, Z.F., Peng, F.J., Huang, G.Y., 2014a. Contamination profiles of perfluoroalkyl substances in five typical rivers of the Pearl River Delta region, South China. *Chemosphere* 114. <https://doi.org/10.1016/j.chemosphere.2014.04.005>.

Pan, C.G., Ying, G.G., Zhao, J.L., Liu, Y.S., Jiang, Y.X., Zhang, Q.Q., 2014b. Spatiotemporal distribution and mass loadings of perfluoroalkyl substances in the Yangtze River of China. *Sci. Total Environ.* 493, 580–587. <https://doi.org/10.1016/j.jscitotenv.2014.06.033>.

Pan, Y., Zhang, H., Cui, Q., Sheng, N., Yeung, L.W.Y., Sun, Y., Guo, Y., Dai, J., 2018. Worldwide distribution of novel perfluoroether carboxylic and sulfonic acids in surface water. *Environmental Science & Technology* 52 (14), 7621–7629. <https://doi.org/10.1021/acs.est.8b00829>.

Pignotti, E., Casas, G., Llorca, M., Tellbüscher, A., Almeida, D., Dinelli, E., Farré, M., Barceló, D., 2017. Seasonal variations in the occurrence of perfluoroalkyl substances in water, sediment and fish samples from Ebro Delta (Catalonia, Spain). *Sci. Total Environ.* 607–608. <https://doi.org/10.1016/j.scitotenv.2017.07.025>.

Podder, A., Sadmani, A.H.M.A., Reinhart, D., Chang, N.B., Goel, R., 2021. Per and poly-fluoroalkyl substances (PFAS) as a contaminant of emerging concern in surface water: a transboundary review of their occurrences and toxicity effects. *J. Hazard Mater.* 419. <https://doi.org/10.1016/j.jhazmat.2021.126361>.

Rankin, K., Mabury, S.A., Jenkins, T.M., Washington, J.W., 2016. A North American and global survey of perfluoroalkyl substances in surface soils: distribution patterns and mode of occurrence. *Chemosphere* 161. <https://doi.org/10.1016/j.chemosphere.2016.06.109>.

Reinikainen, J., Perkola, N., Äystö, L., Sorvari, J., 2022. The occurrence, distribution, and risks of PFAS at AFFF-impacted sites in Finland. *Sci. Total Environ.* 829. <https://doi.org/10.1016/j.scitotenv.2022.154237>.

Ruan, T., Lin, Y., Wang, T., Liu, R., Jiang, G., 2015. Identification of novel polyfluorinated ether sulfonates as PFOS alternatives in municipal sewage sludge in China. *Environ. Sci. Technol.* 49 (11). <https://doi.org/10.1021/acs.est.5b01010>.

Sardina, P., Leahy, P., Metzeling, L., Stevenson, G., Hinwood, A., 2019. Emerging and legacy contaminants across land-use gradients and the risk to aquatic ecosystems. *Sci. Total Environ.* 695. <https://doi.org/10.1016/j.scitotenv.2019.133842>.

Sim, W., Park, H., Yoon, J.K., Kim, J.I., Oh, J.E., 2021. Characteristic distribution patterns of perfluoroalkyl substances in soils according to land-use types. *Chemosphere* 276. <https://doi.org/10.1016/j.chemosphere.2021.130167>.

Speight, J.G., 2018. Chapter 7—redox transformations. In: Speight, J.G. (Ed.), *Reaction Mechanisms in Environmental Engineering*. Butterworth-Heinemann, pp. 231–267. <https://doi.org/10.1016/B978-0-12-804422-3.00007-9>.

Steenland, K., Winquist, A., 2021. PFAS and cancer, a scoping review of the epidemiologic evidence. *Environ. Res.* 194, 110690. <https://doi.org/10.1016/J.ENVRES.2020.110690>.

Sun, M., Arevalo, E., Strynar, M., Lindstrom, A., Richardson, M., Kearns, B., Pickett, A., Smith, C., Knappe, D.R.U., 2016. Legacy and emerging perfluoroalkyl substances are important drinking water contaminants in the cape fear river watershed of North Carolina. *Environ. Sci. Technol. Lett.* 3 (12), 415–419. <https://doi.org/10.1021/acs.estlett.6b00398>.

United States Environmental Protection Agency, 2022. Fact sheet: draft 2022 aquatic life ambient water quality criteria for perfluorooctanoic acid (PFOA) and perfluorooctane sulfonic acid (PFOS). www.epa.gov/wqc/aquatic-life-criteria.

U.S. Environmental Protection Agency, 2024. PFAS National Primary Drinking Water Regulation FAQs for Drinking Water Primacy Agencies. https://www.epa.gov/system/files/documents/2024-04/pfas_npwdr_faqsstates_4.8.24.pdf.

US EPA, 2016. Definition and Procedure for the Determination of the Method Detection Limit. US EPA. *Revision 2*. https://www.epa.gov/sites/default/files/2016-12/documents/mdl-procedure_rev2_12-13-2016.pdf.

US Epa, O., 2015. Risk management for per- and polyfluoroalkyl substances (PFAS) under TSCA. <https://www.epa.gov/assessing-and-managing-chemicals-under-tscas-risk-management-and-polyfluoroalkyl-substances-pfas>.

Van Metre, P.C., Alvarez, D.A., Mahler, B.J., Nowell, L., Sandstrom, M., Moran, P., 2017. Complex mixtures of Pesticides in Midwest U.S. streams indicated by POCIS time-integrating samplers. *Environmental Pollution* 220, 431–440. <https://doi.org/10.1016/j.envpol.2016.09.085>.

Wang, S., Huang, J., Yang, Y., Hui, Y., Ge, Y., Larssen, T., Yu, G., Deng, S., Wang, B., Harman, C., 2013. First report of a Chinese PFOS alternative overlooked for 30 years: its toxicity, persistence, and presence in the environment. *Environ. Sci. Technol.* 47 (18). <https://doi.org/10.1021/es401525n>.

Wang, Y., Kim, J., Huang, C.H., Hawkins, G.L., Li, K., Chen, Y., Huang, Q., 2022. Occurrence of per- and polyfluoroalkyl substances in water: a review. *Environmental Science: Water Research & Technology* 8 (6), 1136–1151. <https://doi.org/10.1039/DIEW00851J>.

Xiao, F., 2017. Emerging poly- and perfluoroalkyl substances in the aquatic environment: a review of current literature. *Water Res.* 124, 482–495. <https://doi.org/10.1016/j.watres.2017.07.024>.

Xiao, F., Hanson, R.A., Golovko, S.A., Golovko, M.Y., Arnold, W.A., 2018. PFOA and PFOS are generated from zwitterionic and cationic precursor compounds during water disinfection with chlorine or ozone. *Environ. Sci. Technol. Lett.* 5 (6). <https://doi.org/10.1021/acs.estlett.8b00266>.

Zhang, D.Q., Wang, M., He, Q., Niu, X., Liang, Y., 2020. Distribution of perfluoroalkyl substances (PFASs) in aquatic plant-based systems: from soil adsorption and plant uptake to effects on microbial community. *Environmental Pollution* 257. <https://doi.org/10.1016/j.envpol.2019.113575>.

Zhang, W., Pang, S., Lin, Z., Mishra, S., Bhatt, P., Chen, S., 2021. Biotransformation of perfluoroalkyl acid precursors from various environmental systems: advances and perspectives. *Environmental Pollution* 272, 115908. <https://doi.org/10.1016/j.envpol.2020.115908>.

Zhao, Z., Xie, Z., Tang, J., Sturm, R., Chen, Y., Zhang, G., Ebinghaus, R., 2015. Seasonal variations and spatial distributions of perfluoroalkyl substances in the rivers Elbe and lower Weser and the North Sea. *Chemosphere* 129. <https://doi.org/10.1016/j.chemosphere.2014.03.050>.